

A NEW ASPECTS OF HARD MACHINING USING CBN TOOLS WITH VARIABLE TOOL CORNER RADIUS AND TOOL WEAR EFFECT

Wit Grzesik, Krzysztof Żak

Summary

In this paper some important mechanical cutting characteristics such as cutting forces, specific cutting energy and cutting power were determined when finish turning of hardened 41Cr4 alloy steel and AISI 52100 and JIS-SUJ2 bearing steels using CBN tools with variable tool corner radius based on the experimental study and literature data. The tool corner radius was varied from 400 to 2400 μm and, in addition, flank wear effect was taken into account. Moreover, surface roughness produced by CBN tools with different tool corner radius was compared and surface finish obtained was characterized in terms of potential functional performance. As a result, the changes of Ra and Rz roughness parameters and relevant material distribution curves and bearing parameters in the form of Symmetrical Curve of Geometrical Contact (SCGC) are presented.

Keywords: hardened steel, tool corner radius, cutting force, specific cutting energy, cutting power, surface roughness

Nowe aspekty skrawania na twarde narzędziami z CBN ze zmiennym promieniem naroża i efektem zużycia ostrza

Streszczenie

W pracy określono niektóre charakterystyki procesu skrawania m.in. składowe siły, energię właściwą i moc skrawania w wykańczającym toczeniu utwardzonej stali stopowej 41Cr4 oraz stali łożyskowej AISI 52100 i JIS-SUJ2 narzędziami z CBN o zmiennym promieniu naroża. W analizie wyników uwzględniono dane doświadczalne i literaturowe. Stosowano promień naroża w zakresie od 400 do 2400 μm . Ustalono również wpływ zużycia ostrza na powierzchni przyłożenia. Dodatkowo, porównano chropowatość powierzchni generowaną ostrzami z CBN o zmiennym promieniu naroża oraz potencjalne właściwości eksploatacyjne powierzchni. Uzyskano zmianę zależności parametrów chropowatości powierzchni Ra i Rz oraz parametrów udziału materiałowego w postaci symetrycznych krzywych kontaktu geometrycznego (SCGC) powierzchni – krzywych Kaczmarka.

Słowa kluczowe: stal utwardzona, promień naroża ostrza, składowe siły skrawania, energia właściwa skrawania, moc skrawania, chropowatość powierzchni, udział materiałowy powierzchni

Address: Prof. Wit GRZESIK, PhD Eng. Krzysztof ŻAK, Faculty of Mechanical Engineering, Opole University of Technology, 5th Mikołajczyka Str., 45-271 Opole, e-mail: k.zak@po.opole.pl, Tel: +48 77 449 8462, Fax: +48 77 449 9927

1. Introduction

Hard machining is a leading machining technology for various highly-loaded machine components made of hardened steels, such as geared shafts, bearing and hydraulic components, with special requirements regarding surface finish and functional performance [1-3]. In general, hard machining process differs from conventional machining process in terms of cutting mechanics, chip formation, tool wear, surface integrity and part accuracy [1, 2]. In particular, manufacturing challenges concern unsatisfactory surface finish and part form accuracy resulting from the specific action of the cutting edge with a high negative rake angle, aggressive thermal influences, rapid tool wear and larger energy consumption [1, 4]. This is due to the fact that the energy consumption increases distinctly due to extreme high hardness of the material machined and high negative rake angle of the CBN cutting tool used. In addition, the tool-workpiece interaction is characterized by severe friction and excessive ploughing action of the cutting edge causing the spring back effect. It is also characteristic that hard machining is performed with dominating passive force in comparison to conventional turning for which the radial force is distinctly lower than the cutting force (typically $F_p = (0.3-0.5)F_c$). As a result, the radial force influences the dynamic behaviour of the machining system and total energy consumption. This specific effect becomes more important when machining with CBN cutting inserts with large nose radius of 800 and 1200 μm or even 2400 (3600) μm [5-7]. As a result, for cutting tools with a corner radius equal to or higher than 1.2 mm uncut chip thickness decreases which intensifies ploughing forces [3, 8]. On the other hand, the roughness height should theoretically decrease when the tool corner radius increases. However, surface finish produced in hard machining deteriorates rapidly when tool wear elevates during several minutes (tool life is relatively short), especially for the cutting speed higher than 120 m/min [9]. Moreover, tool wear influences thermal behaviour of the machining process and, as a result, the retained austenite content and the depth of white layer increase [10, 11]. In order to improve surface finish of machined hard parts the tool corner of ceramic or CBN cutting inserts is modified including large one-radius [1], multi-radii (Wiper geometry) [12] or straight-line fragment parallel to the feed direction [2].

In this study, cutting forces, cutting power consumption, specific cutting energy and surface finish were investigated under the variable tool nose radius in turning of 41Cr5 (AISI 5140) hardened steel. In addition, the experimental data were compared with relevant literature data available in [5-7] obtained in similar hard turning operations with AISI 52100 and JIS-SUJ2 bearing steels.

2. Experimental details

2.1. Workpiece materials

In this investigation hard turning tests were performed using hardened EN 41Cr4 alloy steel with 55 ± 1 HRC hardness. The experimentally obtained data were compared to relevant literature data for both AISI 52100 and JIS-SUJ2 (Japanese equivalent to AISI 52100) bearing steel using fresh and worn CBN cutting tools available in [5,6]. Chemical compositions and mechanical properties of the three steels considered are specified in Tables 1 and 2 respectively.

Table 1. Chemical compositions of the workpiece materials used in comparative study
[<http://www.lucefin.com/en/siderurgia/acciai-speciali-e-al-carbonio>]

Steel grade	Element content, % mas.								
	C	Si	Mn	P	S	Cr	Mo	Al	Cu
EN 41Cr4	0.38- -0.45	max 0.40	0.60- -0.90	max 0.025	max 0.035	0.90- -1.20	max 0.10	max 0.050	max 0.30
AISI 52100	0.93- -1.05	0.15- -0.35	0.25- -0.45	max 0.025	max 0.015	1.35- -1.60	–	–	–
JIS-SUJ2	0.95- -1.10	0.15- -0.35	≤ 0.50	≤ 0.025	≤ 0.025	1.30- -1.60	–	–	–

Table 2. Mechanical properties of the workpiece materials used in comparative study
[<http://www.lucefin.com/en/siderurgia/acciai-speciali-e-al-carbonio>]

Steel grade	Mechanical properties			
	HRC	UTS, N/mm ²	R _{p0.2} , N/mm ²	YS, GPa
EN 41Cr4	55	2080	1590	210
AISI 52100/JIS-SUJ2	60	2470	2190	190-210

2.2. Machining conditions

In the experimental study, CBN cutting tools equipped with TNGA inserts with the corner radius of $r_e = 400, 800$ and $1200 \mu\text{m}$ of CB 7015 grade by Sandvik Coromant were used in hard turning tests with DIN 41Cr4 hardened alloy steel. The chamfer configuration with the rake angle of $\gamma_{cf} = -30^\circ$ and the average cutting edge radius of $r_n = 10 \mu\text{m}$ was selected. Cutting parameters for this part of investigations are specified in Table 3. Machining trials were performed on a three-axis CNC turning center, Okuma Genos model L200E-M. Technological cutting parameters and values of tool corner radius considered in the comparative study extended for AISI 52100 and JIS-SUJ2 bearing steels are specified in Table 3. In particular, also larger corner radiuses of $1600, 2400 \mu\text{m}$ were considered.

Table 3. Specification of machining conditions employed in comparative study

Steel grade	Cutting speed, v_c in m/min	Feed rate, f in mm/rev	Depth of cut, a_p in mm	Tool corner radius, r_ϵ in μm
EN 41Cr4	210	0.1	0.2	400, 800, 1200
AISI 52100	120-180	0.05-0.6	0.2	800, 1600, 2400
JIS-SUJ2	120	0.1	0.2	400, 800, 1200

2.3. Measurements of componential cutting forces and surface roughness

Three components of the resultant cutting force F_c , F_f and F_p were measured using a three-component Kistler dynamometer (model 9129A) and consumed energy recording system installed on the CNC lathe. The measured signals were processed with a sampling rate of $f = 1$ kHz and a low-pass filter with a cut-off frequency of $f_c = 300$ Hz. Surface roughness produced by finish hard turning was measured by means of the stylus method using a Tester 1000 contact profilometer with a diamond stylus tip of $2 \pm 0,5$ μm radius. A set of 2D roughness parameters was determined and surface profiles were visualized using a Digital Surf, Mountains®Map package.

2.4. Computations of specific cutting energy

Specific cutting energy e_c is calculated as the ratio of the measured value of the cutting force F_c and the cross-sectional area of cut which is calculated as the product of the equivalent cutting edge of the length l_k and the mean uncut thickness h_m shown in Fig. 1. The equation is as follows:

$$e_c = F_c / A_c \quad (1)$$

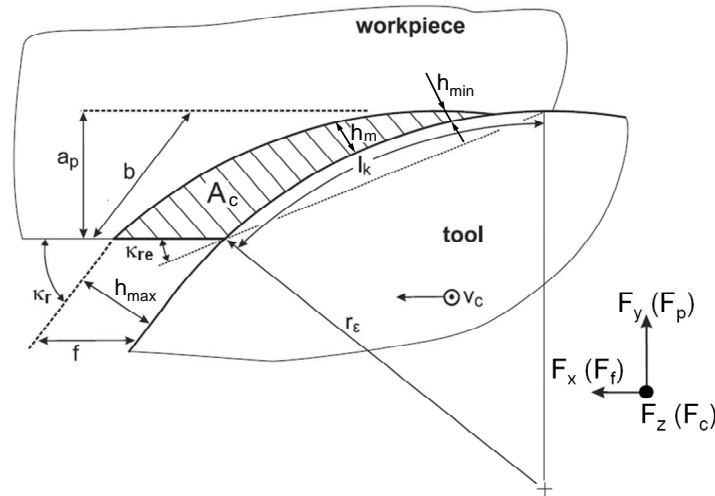


Fig. 1. Typical cross-section of the uncut chip layer for finish hard turning [13]

2.5. Computations of theoretical roughness parameters

The theoretical values of roughness height R_{zt} and average roughness R_{at} were determined using the classical circle model (Eq. 2a) and the corresponding model (Eq. 2b) respectively [2].

$$R_{zt} = \frac{f^2}{8r_\epsilon} \quad (2a)$$

$$R_{at} = \frac{f^2}{31.2r_\epsilon} \quad (2b)$$

3. Experimental results and discussion

3.1. Cutting forces and their relationships

As mentioned above three components F_c , F_f and F_p of the resultant cutting force were recorded during hard turning passes using CBN cutting tool inserts with selected tool corner radiuses and the set of constant machining conditions using a piezoelectric dynamometer. Simultaneously, the cutting power P_c was recorded along with other power components using a special measurement system [4]. The changes of three force components resulting from variations of the tool corner radius are presented in Fig. 2. As shown in Fig. 2 the minimum values of the cutting and passive forces were revealed for the minimum and maximum tool corner radii of 400 and 1200 μm respectively. On the other hand, the minimum values of the feed force were recorded for the medium tool corner radius of 800 μm (Fig. 2). It should be noted in Fig. 2 that the values of passive force recorded in the turning of DIN 41Cr4 and JIS-SUJ2 hardened steel are distinctly higher than the corresponding values of cutting force F_c .

As shown in Fig. 3 the ratio of F_p/F_c varies from 1.10 for lower tool corner radius of $r_\epsilon = 400 \mu\text{m}$ to 1.45-1.55 for higher values of r_ϵ . Its highest value was determined for $r_\epsilon = 800 \mu\text{m}$ and the cutting speed of 210 m/min. This specific force resolution in hard machining causes the relevant changes in power consumption due to an intensive ploughing effect (abnormal value of the passive force F_p) and the generation mechanism of surface roughness. Distinctly higher values of the ratio of F_p/F_c ranging from 1.35 to 1.7 were determined at lower depth of cut of 0.1 mm for JIS-SUJ2 bearing steel. In addition, the values of F_p/F_f ratio exceed the relevant values of the F_p/F_c ratio. This means that the increase of the workpiece material hardness from 55 HRC to 60 HRC also influences the relations between componential forces.

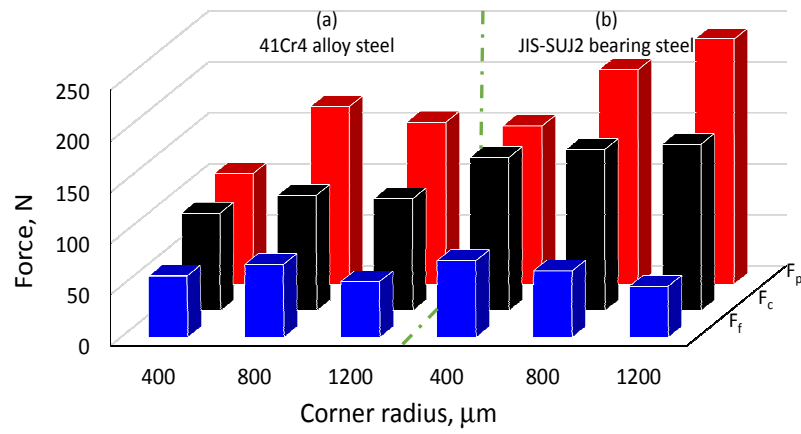


Fig. 2. Influence of tool corner radius on the components of resultant cutting force for (a) 41Cr4 alloy steel with 55 ± 1 HRC hardness, (b) JIS-SUJ2 bearing steel with 60 HRC hardness (experimental data adopted from [6]). Machining conditions: cutting speed $v_c = 210$ m/min (a) and 120 m/min (b), feed rate $f = 0.1$ mm/rev and depth of cut $a_p = 0.2$ mm

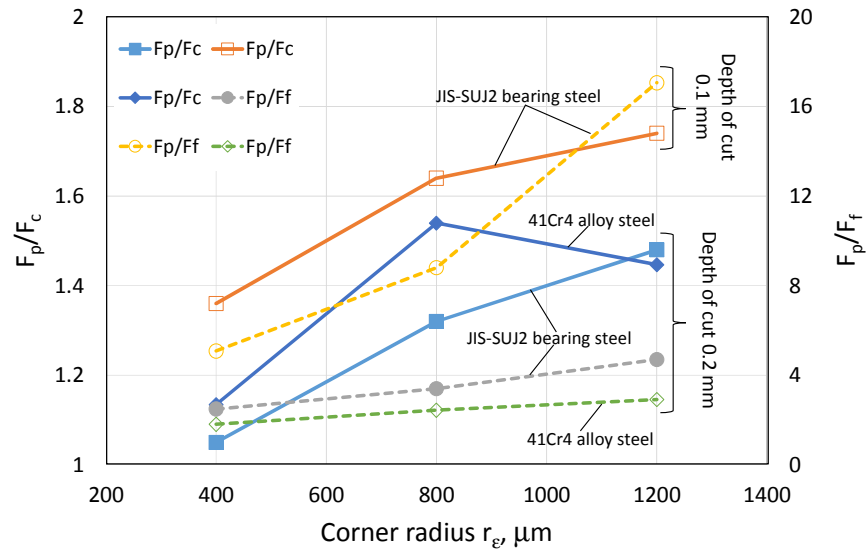


Fig. 3. Influence of tool corner radius and depth of cut on the force ratio F_p/F_c and F_p/F_f for 41Cr4 alloy steel with 55 ± 1 HRC hardness and JIS-SUJ2 bearing steel with 60 HRC hardness (experimental data adopted from [6])

3.2. Changes of specific cutting energy

The changes of the specific cutting energy e_c for fresh and worn CBN cutting tools are illustrated in Figs. 4 and 5 respectively. Figure 4 shows that values of e_c depend on the tool corner radius rather for lower feed rates and vary in a similar way to the changes of relevant cutting forces.

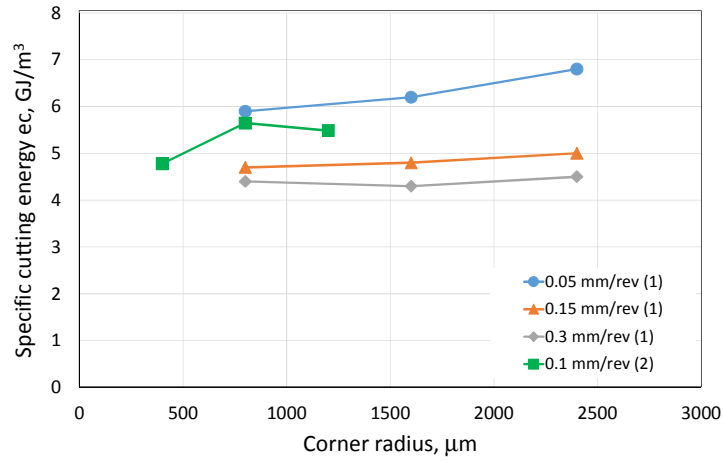


Fig. 4. Influence of tool corner radius and feed rate on the specific cutting energy for fresh tools. Legend: (1) $v_c = 120$ m/min, $a_p = 0.2$ mm AISI 52100 (experimental data adopted from [5]), (2) $v_c = 210$ m/min, $f = 0.1$ mm/rev, $a_p = 0.2$ mm 41Cr4

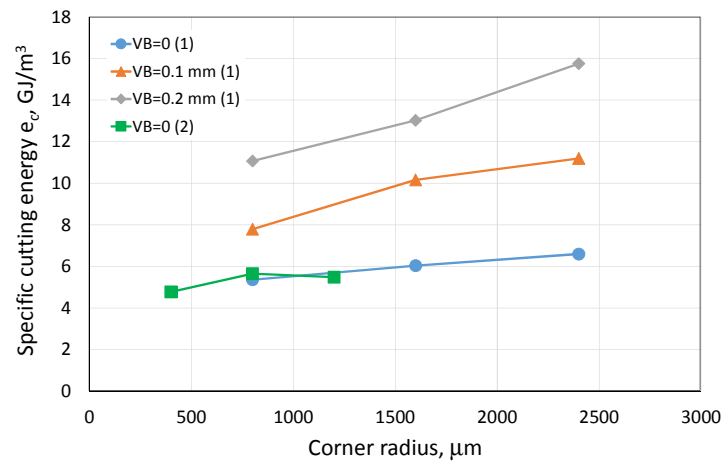


Fig. 5. Influence of tool corner radius and tool wear on the specific cutting energy for AISI 52100 bearing steel with 60-62 HRC hardness. Legend: (1) $v_c = 180$ m/min, $f = 0.05$ mm/rev, $a_p = 0.2$ mm for AISI 52100 steel (experimental data adopted from [5]), (2) $v_c = 210$ m/min, $f = 0.1$ mm/rev, $a_p = 0.2$ mm for 41Cr4 steel

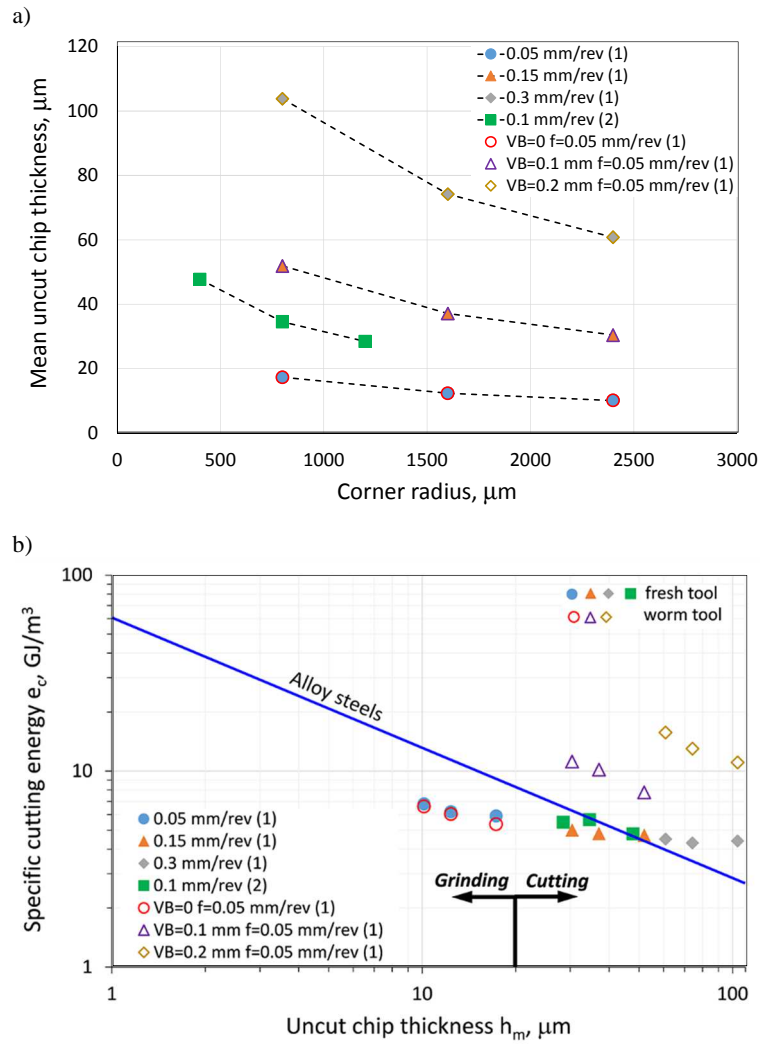


Fig. 6. Changes of UCT vs tool corner radius for different feed rates (a). and specific cutting energy vs. uncut chip thickness in log-log scale for fresh and worn tools for EN 41Cr4 and AISI 52100 steels with alloy steels as a reference workpiece material (b). Legend: (1) $v_c = 120 \text{ m/min}$, $f = 0.05 \text{ mm/rev}$, $f = 0.15 \text{ mm/rev}$, $f = 0.3 \text{ mm/rev}$, $a_p = 0.2 \text{ mm}$ for AISI 52100 steel, (2) $v_c = 210 \text{ m/min}$, $f = 0.1 \text{ mm/rev}$, $a_p = 0.2 \text{ mm}$ for 41Cr4 steel

The minimum values of $e_c = 4.6\text{-}5.9 \text{ GJ/m}^3$ were recorded for the tool corner radius of 400 and 800 μm . The specific cutting energy increases slightly for higher feed rates and more intensively (on average by 15%) for lower feed rates applied. As a result, the specific energy determined for fresh cutting tools does not exceeds 7 GJ/m^3 when tool corner radius increases from 400 μm to 2400 μm .

As shown in Fig. 5 the progress of tool wear from $VB_B = 0.1$ mm to $VB_B = 0.2$ mm causes that the values of the specific cutting energy (SCE) increase distinctly about two or three times respectively in comparison to fresh tools denoted by flank wear indicator $VB_B = 0$. In contrast to fresh tools the highest increase of SCE is observed for worn tools with the flank wear of $VB_B = 0.2$ mm.

In general, as presented in Fig. 6a, the uncut chip thickness (UCT) depends on the feed rate applied and geometrically (Fig. 1) on the tool corner radius. As a result, machining with lower feed rates and higher corner radiuses cause that the UCT decreases substantially down to several microns (to about $10 \mu\text{m}$ for $f = 0.05$ mm/rev and $r_\epsilon = 2400 \mu\text{m}$). As shown in Fig. 6b the specific cutting energy for a lower tool corner radius is in the range characteristic for grinding with the uncut chip thickness (UCT) of about $15 \mu\text{m}$ (Fig. 6a) and for higher tool corner radius is in the range characteristic for conventional turning of alloy steels with the UCT higher than $20 \mu\text{m}$ [2,13]. However, the specific cutting energy increases visibly when flank wear increases up to $VB_B = 0.2$ mm. In case of worn cutting tools the specific cutting energy ranges from 8-16 GJ/m³ depending on the tool corner radius and flank wear progress. As a result, the generation of white layer is also intensified [5,10].

3.3. Changes of cutting power

The changes of the cutting power determined as the product of $P_c = F_c \times v_c$ recorded for different tool corner radiuses are shown in Figs. 7, 8 and 9. The trends are similar to those observed for the cutting force F_c (Fig. 2) when keeping constant cutting speed. As shown in Fig. 7a, the difference between the calculated and measured values of the cutting power is not higher than 10%. Moreover,

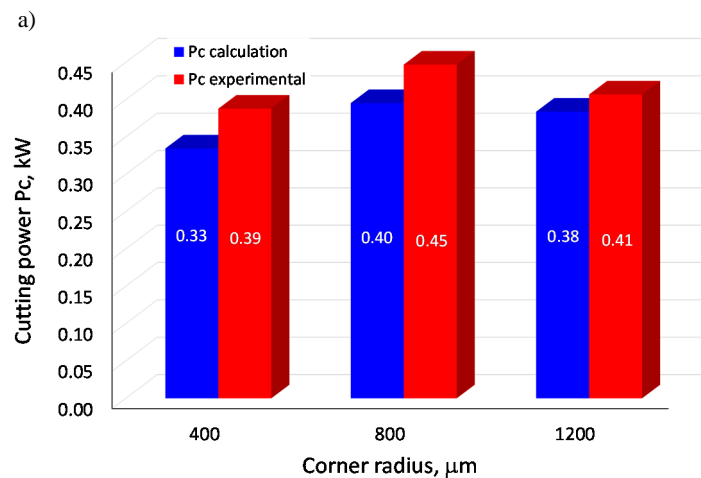


Fig. 7. Changes of cutting power for variable tool nose radius and cutting speed (a)

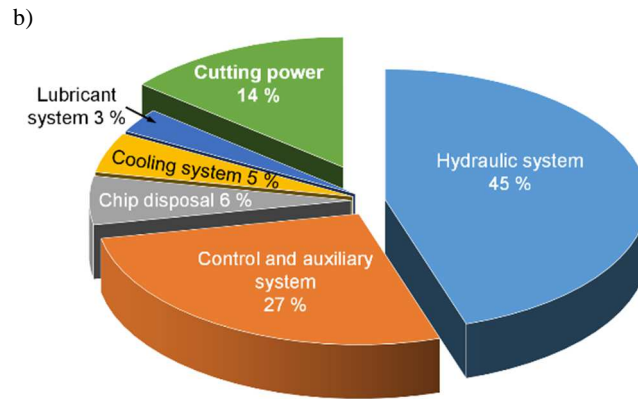


Fig. 7. Changes of cutting power for variable tool nose radius and cutting speed (a) and pie diagram of power distribution for a three-axis CNC turning center, Okuma Genos model L200E-M for $v_c = 210$ m/min, $f = 0.1$ mm/rev, $a_p = 0.2$ mm [4] (b)

power consumption resulting from employing CBN tools with the tool corner radius of $r_\epsilon = 800$ and 1200 μm differs only by about 2-5%. The pie diagram presented in Fig. 7b indicates that in hard machining the power consumption strictly for cutting performance is about 14% of the total power recorded independently of the tool corner selected in this comparative studies.

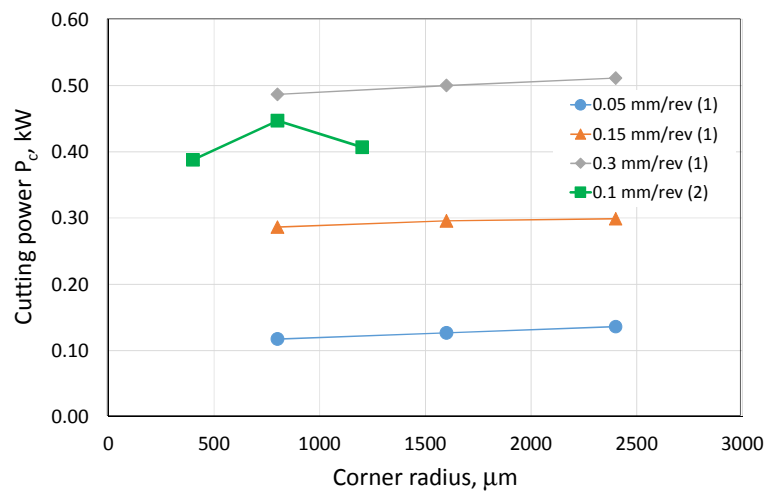


Fig. 8. Influence of tool corner radius and feed rate on the cutting power for fresh tools. Legend: (1) $v_c = 120$ m/min, $a_p = 0.2$ mm for AISI 52100 (experimental data adopted from [5]), (2) $v_c = 210$ m/min, $f = 0.1$ mm/rev, $a_p = 0.2$ mm for DIN 41Cr4

Influence of tool corner radius on the cutting power for fresh and worn cutting tools is presented in Figs. 8 and 9 respectively. The main observations are that the cutting power for worn tools is more sensitive for changes of the tool corner radius and the cutting power increases of about 30% when it increases from 400 to 2400 μm (see Fig. 9). On the other hand, the appropriate changes of P_c determined for fresh tools are rather small and do not exceed 5%. It should be noted based on the dependence of the cutting power on the tool corner radius (Fig. 8 vs Fig. 9) that lower values of P_c were determined for worn tools. This specific effect can be explain in terms of the crater wear of chamfered CBN tools which causes that the effective rake angle decreases and, as the result, the corresponding cutting force and resulting cutting power decreases [14].

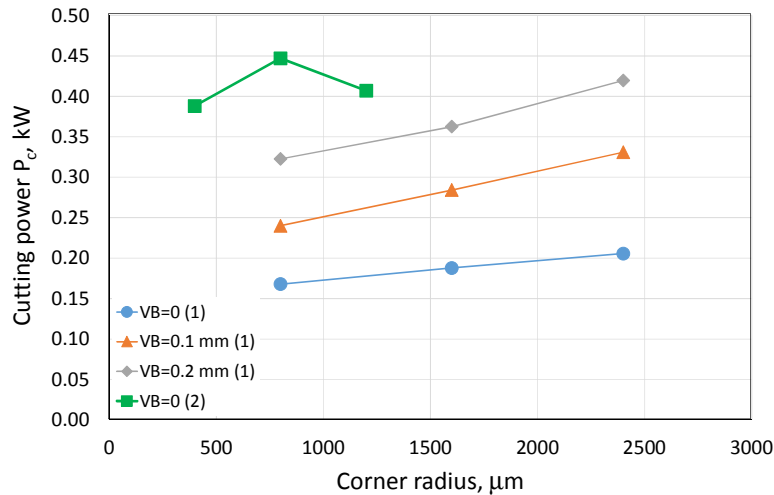


Fig. 9. Influence of tool corner radius on cutting power for worn tools. Legend: (1) $v_c = 180$ m/min, $f = 0.05$ mm/rev, $a_p = 0.2$ mm AISI 52100 (experimental data adopted from [5]), (2) $v_c = 210$ m/min, $f = 0.1$ mm/rev, $a_p = 0.2$ mm 41Cr4

4. Surface roughness

4.1. Changes of surface profile

Representative surface profiles generated by CBN tools with different tool nose radius are shown in Fig. 10. It can be observed in Fig. 10 that the surface profile is smoothed when using cutting tools with higher tool corner radius. Another specific effect resulting from employing CBN tools with a large tool corner is a visible reduction of the RMS slope $R\Delta q$ from 4.37° for $r_\epsilon = 400$ μm up to 1.67° for $r_\epsilon = 1200$ μm (Fig. 10).

Surface profiles presented in Fig. 10a-c contain regular feed marks but the most regular (determined) surface profile is produced when using CBN tool with the minimum $r_\epsilon = 400 \mu\text{m}$. When the tool corner radius increases feed marks are slightly distorted probably by small side flows observed on the left sides of all individual peaks (see Fig. 10c). They appear due to the lateral plastic flow which occurs when the cutting edge removes a very thin layer of thermally softened material [10].

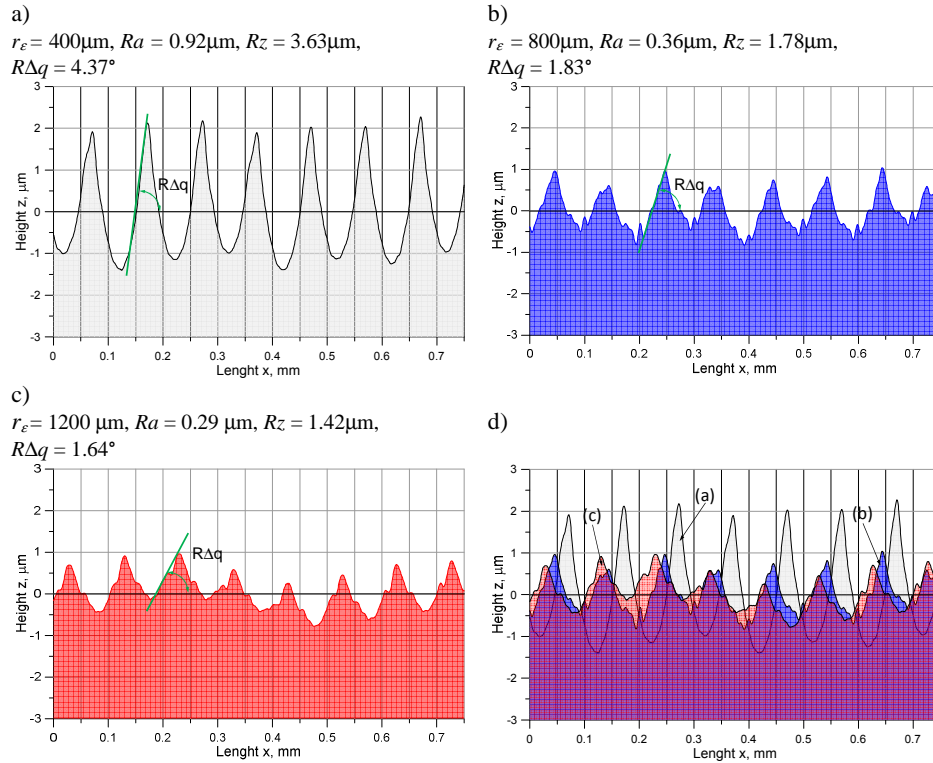


Fig. 10. Comparison of surface profiles generated by CBN tools with different tool corner radius for $v_c = 210 \text{ m/min}$, $f = 0.1 \text{ mm/rev}$ and $a_p = 0.2 \text{ mm}$

4.2. Changes of surface roughness parameters and functional indexes

As shown in Fig. 11a the maximum roughness height R_z decreases from $3.6 \mu\text{m}$ for $r_\epsilon = 400 \mu\text{m}$, through 1.8 for $r_\epsilon = 800 \mu\text{m}$ to $1.5 \mu\text{m}$ for the highest $r_\epsilon = 1200 \mu\text{m}$. It can also be noted that the relevant values of the average roughness R_a decrease down to 0.9 , 0.4 and $0.3 \mu\text{m}$ respectively. In addition, the real values of both R_a and R_z roughness parameters can be predicted with a reasonable accuracy using Eqns. 2a and 2b but better prediction results concern the average

roughness R_a . This is due to fact that the predicted values of R_z parameter should be additionally corrected by appropriate elastic recovery (*springback*) of the machined surface [15].

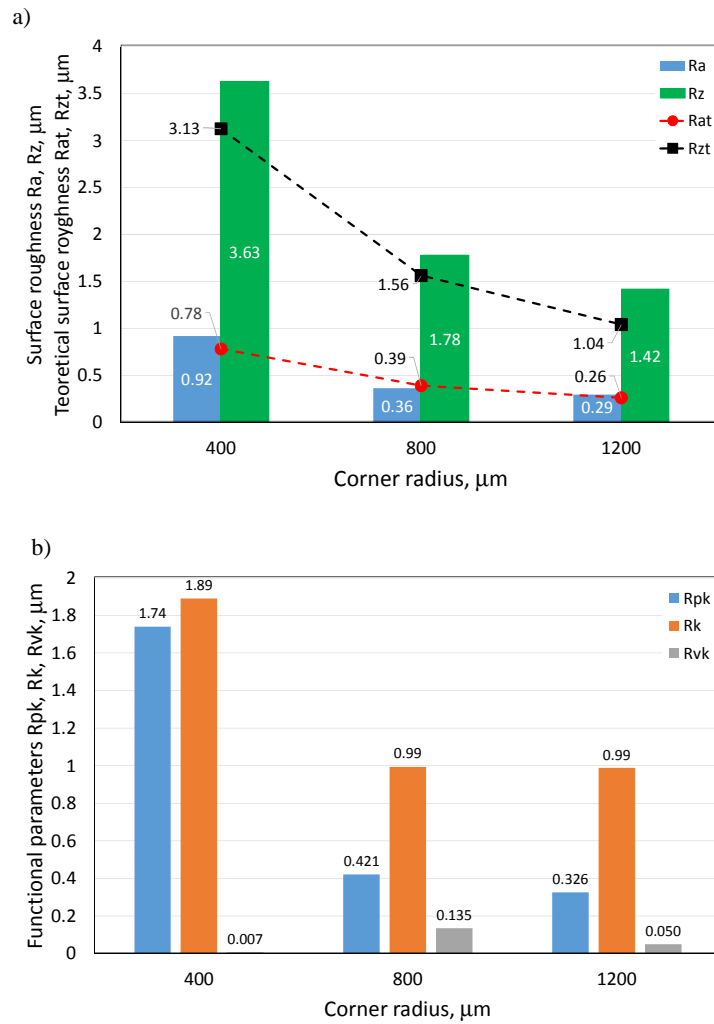


Fig. 11. Changes of R_a and R_z roughness parameters (a) and R_{pk} , R_k and R_{vk} bearing parameters (b) for variable tool corner radius ($v_c = 210$ m/min, $f = 0.1$ mm/rev, $a_p = 0.2$ mm)

The effect of tool nose radius on the surface profile can also be pronounced when considering the bearing parameters R_{pk} , R_k and R_{vk} , as shown in Fig. 11b. In general, this influence concerns the reduced peak height R_{pk} and the reduced core height R_{vk} . In both cases presented in Fig. 11a and b some surface roughness

parameters decreases when the tool corner radius increases from 400 to 800 μm . The visualization of the influence of tool nose radius on the bearing properties of the surface profile is also presented in the form of SCGC diagrams in Fig. 12b.

Figure 12a confirms that CBN hard turning produced surface profiles with unsatisfactory bearing properties but the increase of the tool corner ratio causes that the profiles of material ratio curve (MRC) changes from fully degressive for the minimum corner radius of $r_{\epsilon} = 400 \mu\text{m}$ to progressive-degressive for higher tool corner radii of $r_{\epsilon} = 800$ and $1200 \mu\text{m}$. The most important is that the increase of tool corner radii does not influence the material ratio at the cut above 70%.

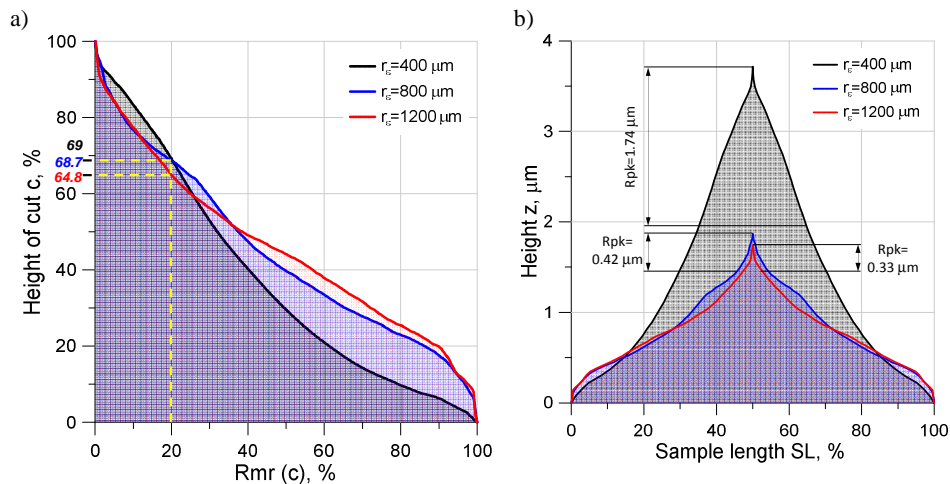


Fig. 12. Changes of the shapes of material ratio curves (a) and SCGC diagrams (b) for variable tool corner radius ($v_c = 210 \text{ m/min}$, $f = 0.1 \text{ mm/rev}$, $a_p = 0.2 \text{ mm}$)

This is in accordance with relevant changes of Rpk , Rk and Rvk bearing parameters shown in Fig. 11b. In particular, the reduced peak height Rpk decreases markedly from $1.75 \mu\text{m}$ to about $0.3 \mu\text{m}$ whereas at the same time the reduced valley height Rvk increases from about $0.03 \mu\text{m}$ to about $0.1 \mu\text{m}$. In particular, the reduction of peak height down to $0.3 \mu\text{m}$ observed for surface profiles generated by CBN tools with higher corner radii of $1200 \mu\text{m}$ implies shorter running-time period during the surface's service. The influence of tool corner radius on the resistance of the produced surfaces to abrasive wear is visualized using relevant SCGC diagrams shown in Fig. 12b. On the other hand, the reduced core height remains relatively high of about $1 \mu\text{m}$.

5. Conclusions

- Tool corner radius is a decisive factor influencing such cutting characteristics as components of the resulting cutting force, specific cutting energy and cutting power consumption and controlling surface roughness produced. This complex effect should be considered in terms of tool wear due to relatively low tool life.

- In hard turning the passive force (F_p) overestimates markedly both cutting (F_c) and feed (F_f) forces. For the tool corner radius ranging from 400 μm to 2400 μm the ratio of F_p/F_c increase from 1.10 to about 1.5. It is also influenced by the hardness of machined material.

- The tool corner radius influences the specific cutting energy (SCE). For fresh cutting tools SCE does not exceeds 7 GJ/m^3 but for worn cutting tools the specific cutting energy ranges from 8-16 GJ/m^3 depending on the tool corner radius and flank wear progress.

- The cutting power consumption depends on the cutting tool configuration and its flank wear. The cutting power for worn tools is more sensitive for changes of the tool corner radius and it increases of about 30% when the radius increases from 400 to 2400 μm .

- Distinctly lower values of R_a and R_z roughness parameters were measured on hard surfaces machined using CBN chamfered cutting tools with higher tool corner radius of 800 μm and 1200 μm . The surface profiles are generated with regular feed marks and visible flashes due to plastic side flow effect. As a result, the values of real R_z and R_a roughness parameters can be predicted with a reasonable accuracy, especially for R_a parameter, using simple theoretical formulae.

References

- [1] J.P. DAVIM (ed.): Machining of hard materials. Springer, London 2011.
- [2] W. GRZESIK: Advanced machining processes of metallic materials. Elsevier, Amsterdam 2017.
- [3] W. GRZESIK: Prediction of the functional performance of machined components based on surface topography: State of the art. *Journal of Materials Engineering and Performance*, **25**(2016), 4460-4468.
- [4] R. CHUDY, W. GRZESIK: Comparison of power and energy consumption for hard turning and burnishing operations of 41Cr4 steel. *Journal of Machine Engineering*, **14**(2015), 113-120.
- [5] Y.K. CHOU, H. SONG: Tool nose effects on finish hard turning. *Journal of Materials Processing Technology*, **148**(2004), 259-268.
- [6] M. LIU, J. TAKAGI, A. TSUKUDA: Effect of tool nose radius and tool wear on residual stress distribution in hard machining of bearing steel. *Journal of Materials Processing Technology*, **150**(2004), 234-241.

- [7] J.D. THIELE, S.N. MELKOTE: Effect of cutting edge geometry and workpiece hardness on surface generation in the finish hard turning of AISI 52100 steel. *Journal of Materials Processing Technology*, **94**(1999), 216-226.
- [8] R. MAYER, J. KÖHLER, B. DENKENA: Influence of the tool corner radius on the tool wear and process forces during hard turning. *International Journal of Advanced Manufacturing Technology*, **58**(2012), 933-940.
- [9] M.A. YALLESE, K. CHAOUI, L.B. ZEGHIB, J. F. RIGAL: Hard machining of hardened bearing steel using cubic boron nitride tool. *Journal of Materials Processing Technology*, **209**(2009), 1092-1104.
- [10] G. BARTARYA, S.K. CHOUDHURY: State of the art in hard turning. *International Journal of Machine Tools and Manufacture*, **53**(2012), 1-14.
- [11] S.B. HOSSEINI, T. BENO, U. KLEMENT, J. KAMINSKI, K. RYTTBERG: Measurements and effects on white layer formation in AISI 52100. *Journal of Materials Processing Technology*, **214**(2014), 1293-1300.
- [12] W. GRZESIK, T. WANAT: Comparative assessment of surface roughness produced by hard machining with mixed ceramic tools including 2D and 3D analysis, *Journal of Materials Processing Technology*, **169**(2005), 364-371.
- [13] W. GRZESIK, B. DENKENA, K. ŻAK, T. GROVE, B. BERGMANN: Energy consumption characterization in precision hard machining. *International Journal of Advanced Manufacturing Technology*, **85**(2016), 2839-2845.
- [14] W. GRZESIK, K. ŻAK: Friction quantification in the oblique cutting with CBN chamfered tools. *Wear*, **304**(2013), 36-42.
- [15] W. GRZESIK: Generation and modelling of surface roughness in machining using geometrically defined cutting tools, in: *Metal Cutting. Research Advances*, Nova Science Publishers, New York 2010, 163-185.

Received in December 2016